engineering proceedings

MDPI

Proceeding Paper

Fatigue Testing and Analysis of Flare Bevel Groove-Welded Aluminum Joints for Pedestrian Bridge Applications †

Abdullah Abdelbadie and Scott Walbridge *

Department of Civil and Environmental Engineering, University of Waterloo, Waterloo, ON N2L 3G1, Canada; a4abdelb@uwaterloo.ca

* Correspondence: swalbrid@uwaterloo.ca

† Presented at the 15th International Aluminium Conference, Québec, QC, Canada, 11–13 October 2023.

Abstract: Flare bevel groove (FBG) welds are used in truss bridges with square hollow structural section (HSS) members. To reduce costs, joints can be welded without bevelling, but this negatively impacts the fatigue performance of the connection. This approach is often used in pedestrian bridges made from steel or aluminum. To investigate the fatigue performance of FBG welds, a study was conducted on T-joints made from aluminum square HSS members. The goal was to establish an S–N curve for these welds and present a numerical fatigue life prediction methodology. The study involved cyclic tests supplemented by a fatigue life prediction using linear elastic fracture mechanics (LEFM) coupled with finite element (FE) analysis using the software ABAQUS. Several parameters were varied, including the HSS section size and the corner radius (as extruded and hand ground). Six identical samples were tested for each combination of parameters to generate an S–N curve. The paper ends by drawing conclusions regarding the fatigue performance of aluminum FBG welds and their suitability for use in cyclically loaded structures such as pedestrian bridges.

Keywords: fatigue; flare bevel groove welds; hollow structural sections; aluminum; linear elastic fracture mechanics; finite element analysis

Citation: Abdelbadie, A.; Walbridge, S. Fatigue Testing and Analysis of Flare Bevel Groove-Welded Aluminum Joints for Pedestrian Bridge Applications. *Eng. Proc.* **2023**, *43*, 46. https://doi.org/10.3390/engproc2023043046

Academic Editor: Nicolas Boissonnade

Published: 7 October 2023

1. Introduction

Partial joint penetration welds (PJP) are welds that do not extend fully through the thickness of the material being joined. Instead, the weld only penetrates part of the way through the material. PJP welds are often used in situations where a full penetration weld is not required, such as in joints where the stress on the weld is not significant or where significant cyclic loading is not anticipated. Partial penetration flare bevel groove (FBG) welds can offer some benefits in hollow structural section (HSS) truss construction, such as reduced fabrication costs and faster construction times. If fatigue performance is a critical consideration for a given application, it is generally recommended to use bevelled, full penetration welds. Unfortunately, the literature does not provide much guidance for the fatigue design of PJP welds in general and aluminum FBG welds in particular.

Against this background, the objectives of the project presented in this paper are as follows:

1. to perform fatigue tests on aluminum HSS T-joints with partial penetration FBG welds;
2. to use various existing methods to predict the fatigue performance of these welds.

2. Background

2.1. Fatigue Analysis of PJP Welds in Steel

Studies concerned with PJP welds mostly focus on steel in butt joint applications. For example, refs. [1–3] investigate the effect of the lack of penetration of the weld on the fatigue performance. Ref. [1] investigates the effect of the seam size for partial penetration single- and double-sided welds, which are not permissible for fatigue prone applications, and

investigates their fatigue performance. The study concludes that the fatigue performance of the PJP weld can be evaluated using the stress notch approach with reasonable accuracy, and depending on the seam size, practical applications exist where the cost-saving advantage of these welds can be leveraged while maintaining safety. Refs. [2–4] conduct an experimental study on PJP steel butt welds and conclude that as the lack of penetration increases, the fatigue performance decreases. The results from a fracture mechanics study in [4] show that the fatigue life of the connection can be evaluated successfully for different levels of penetration.

2.2. PJP Weld in Aluminum

The fatigue performance of 6061 aluminum PJP butt joints is investigated through testing and analysis in [5]. The experimental program consists of 56 fatigue life tests at varying degrees of penetration. A fracture mechanics model is used to represent the crack behaviour of the specimen. The study investigates the effect of the heat-affected zone, weld roughness, and lack of penetration. One hundred butt-welded aluminum specimens made from 5083 alloy are tested in [6] with varying thickness and degree of penetration. Applications involving vehicle components are investigated in [6–8]. The conclusions drawn from these studies can be summarized as follows:

- While the fatigue performance of otherwise identical components (measured in terms of externally applied load or nominal stress) decreases with an increase in the degree of penetration [6,8], the influence of the degree of penetration is predictable if the employed stress definition considers the net weld cross section and is measured accurately [5];
- Certain fabrication defects such as eccentricity from warping can detrimentally reduce the fatigue performance of the connection [8];
- The base metal thickness has little influence on fatigue performance [6,8].

3. Experimental Program

This section summarizes the experimental program undertaken for this project, which investigates the fatigue performance of partial penetration FBG welds between aluminum HSS sections, as would commonly be used in applications such as pedestrian bridges.

3.1. Description of Experimental Program

The experimental program consisted of 32 specimens divided into four groups (see Table 1) with varied parameters including HSS section size and corner radius (as extruded and hand ground). Six samples were fabricated for each combination of parameters and tested at varying load ranges to generate an S–N curve for each geometry. Two specimens of each geometry group (8 of the total 32) were tested to find out the static strength of each geometry, while the remaining 24 specimens were fatigue tested to generate the design S–N curve. Determining the static strength of the specimen was necessary to identify a reasonable load range for the fatigue testing. The fatigue load ranges that were applied varied between 30% and 50% of the static strength. A load ratio (R = minimum load/maximum load) of 0.2 was used for all of the tests. The specimens consisted of welded aluminum HSS T-joints with properties summarized in Figure 1.

Table 1. Specimen dimensions as defined in Figure 1.

Sample Name	Corner Radius	L1 (mm)	L2 (mm)	W (mm)	t (mm)
R-4.8	4.8	300	350	75	6.4
R-11.1	11.1	300	350	75	6.4
R-12.7	12.7	300	450	100	12.7
R-HG	HG	300	650	100	12.7

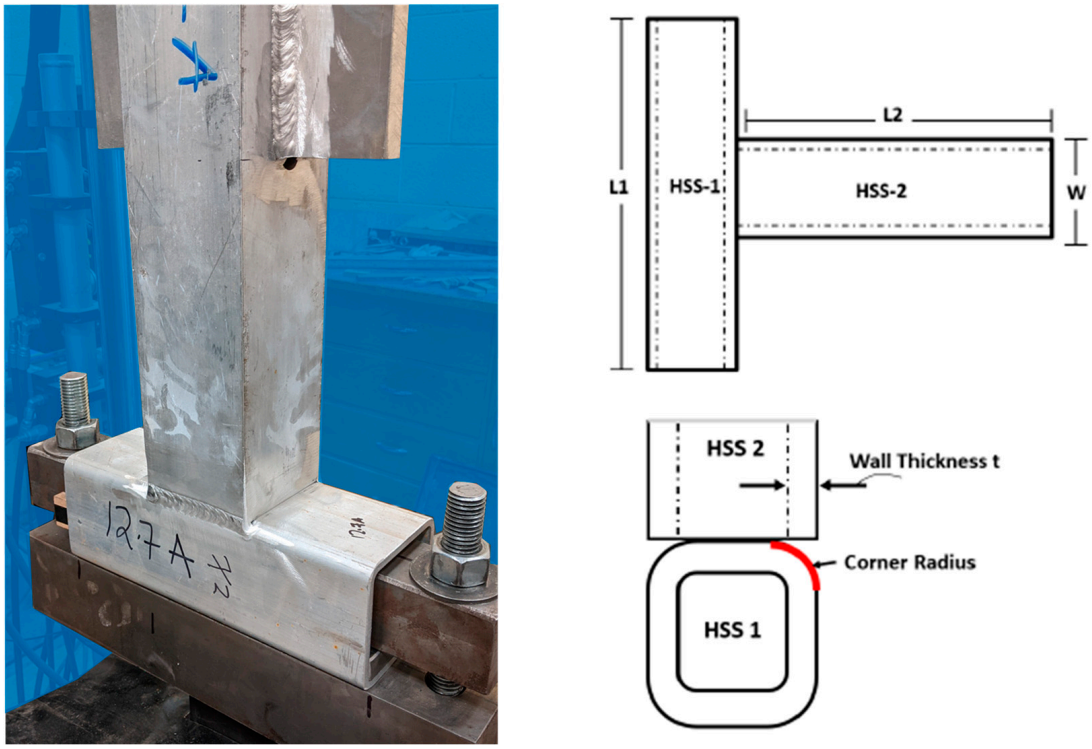

Figure 1. Specimen geometry and dimension definitions.

3.2. Experimental Results

Only 20 of the 24 fatigue-tested specimens were included in the fatigue analysis because of complications that occurred in the lab, fatigue runouts, and failures not occurring in the weld. The following is a summary of the omitted tests and their respective modes of failure:

Two specimens were "runouts" (i.e., did not fail);

One specimen failed due to an error in calibrating the loading frame;

One specimen failed via tear-out of the bottom of the HSS due to the use of a small-size steel fixture bar which caused additional bending in the tube wall.

The statistical analysis performed for this study of the fatigue performance of the tested FBG welds was based solely on the results obtained from the remaining 20 tests. In Figure 2, the test results are plotted on a log–log stress-life (S–N) plot with the detail categories used by the Aluminum Design Manual [9], CSA S157 [10], and S6 [11] plotted for comparison. It should be mentioned that in this figure, the stress is obtained by dividing the load by the measured net section through the weld throat. Looking at this figure, it would appear that the HSS member size and the grinding of the tube corners had relatively insignificant effects on the results. The scattered and dominant trend in the results indicates that the main parameter of influence on the performance of a specimen is the level of stress in the weld. The size of the effective throat is dictated primarily by the corner radius of the HSS member; the larger the corner radius, the larger the area of the partial penetration weld, and therefore, the lower the stress on the net section for a given load level.

When analyzing the results of the fatigue tests for the purpose of generating a design S–N curve, a line of best fit must first be generated to describe the trend of this data. The line of best fit is afterwards used to generate a design curve which guarantees a predetermined survival probability (95% is used in most international standards or 97.7%—two standard deviations below the mean—in the North American standards). The design curve will afterwards be used to relate the fatigue performance of the welded configuration to one of the standard detail categories. The statistical analysis that was used to generate the line of

best fit and design curve was the guideline for analysis of fatigue data published by the International Institute of Welding (IIW) [12].

As shown in Figure 3, the result of this exercise for the tests conducted in this study is a design curve associated with a 95% survival probability, falling very close to the Category E design curve. This means if an engineer is looking for a way to easily analyze the fatigue performance of FBG welds for aluminum T-joints or similar structural configurations, then they can simply refer to the Category E S–N curve and locate the stress range corresponding to the desired fatigue life. An important point to note is that the stress in Figures 2 and 3 is based on the measured throat. In real structures, the throat size is not known. Additional analysis (omitted here for brevity) found a much higher degree of scatter in the data when a design throat was used instead of measured throat to calculate the fatigue stress range used to generate the S–N data.

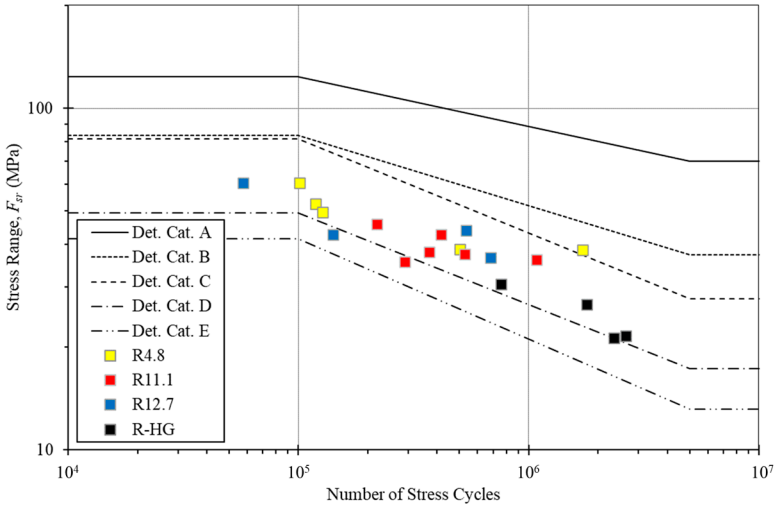

Figure 2. Test results (area used to calculate the stress based on measured effective throat).

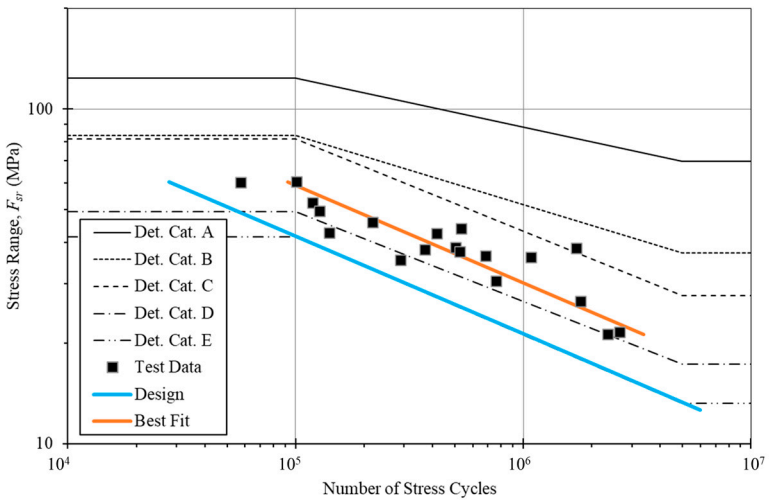

Figure 3. Statistical analysis of fatigue tests (stress based on measured throat).

4. Analysis of Results

This section summarizes an analysis of the partial penetration FBG weld tests presented in Section 3 using linear elastic fracture mechanics (LEFM). In the following paragraphs, the theory and tools used to conduct this analysis are first reviewed; the results are then presented.

4.1. Linear Elastic Fracture Mechanics (LEFM)

Linear elastic fracture mechanics (LEFM) provides a mathematical approach for the prediction of crack growth and fracture in materials subjected to fatigue loading. The approach is based on the concept of a stress intensity factor (SIF) which describes the intensity of the stress at the tip of a crack. The SIF is used to calculate the rate of crack growth which can be related to the number of cycles to fracture. This approach is advantageous because it does not rely on the use of empirical S–N data. The Paris–Erdogan law relates the crack growth rate to the applied SIF range. The relationship between the crack growth rate and the SIF range, ΔK, provides a means of predicting the progression of a crack. However, it is important to note that the law is only valid for small crack growth rates and for materials operating in the linear-elastic domain.

According to this law, the crack growth rate, da/dN, is proportional to ΔK^m:

$$\frac{da}{dN} = C \cdot \Delta K^m, \tag{1}$$

where C and m are material constants obtained by testing or from the literature [13].

Upon integrating Equation (1), the fatigue life, N_f, is taken as:

$$N_f = \int_{a_0}^{a_f} \frac{da}{C\,(\Delta K_{eff}^m - \Delta K_{th}^m)}, \tag{2}$$

where a_f is the crack size that causes failure. This is calculated as:

$$a_f = \frac{t}{2}\left(1 - \frac{\rho_0\,\Delta\sigma_n}{\sigma_u(1-R)}\right), \tag{3}$$

where ρ_0 is the degree of penetration and t is the thickness of the material.

a_0 is the initial crack size and is calculated as:

$$a_0 = t(1-\rho_0). \tag{4}$$

ΔK_{th} is the threshold value for the SIF range that separates the crack initiation and crack propagation regimes. Geometric and loading conditions that result in $\Delta K_{eff} < \Delta K_{th}$ will cause no crack propagation. ΔK_{th} is a material-dependent property that can either be obtained experimentally through conducting a crack propagation test or through the literature. For this study, ΔK_{th} for aluminum is obtained from the IIW Recommendations [12] and taken as:

$$\Delta K_{th} = 56.7 - 72.3R \ \geq 21. \tag{5}$$

If the load ratio, R, is equal to 0.2 then $\Delta K_{th} = 42.24\ \text{MPa}\sqrt{\text{mm}}$.

ΔK_{eff} is the effective stress intensity range calculated by multiplying the difference between the stress intensity factors resulting from the maximum and minimum loads applied in each load cycle (K_{Max} and K_{Min}) with a factor, U, which accounts for crack closure effects:

$$\Delta K_{eff} = (K_{Max} - K_{Min}) \cdot U. \tag{6}$$

Crack closure refers to the phenomenon in which crack opening is partially delayed by the interaction between the crack faces and the surrounding material. This interaction can result in a reduction in the stress intensity factor (SIF) at the crack tip. Plastic deformation of the material near the crack tip can result in partial closure of the crack even when it is subjected to tensile loading. Consideration of crack closure results in a more realistic representation of the crack behaviour, while yielding a less conservative fatigue life prediction. Various methods exist to model crack closure, including yield strip models and simple linear relationships. However, a method was proposed by Newman et al. [14] mathematically relating stress to the crack closure factor, U. This method was modified by McClung [15] by replacing the stress terms in the equations with stress intensity factor

terms. The modified method proposed by McClung has been chosen for this study because it has been successfully used to analyze cracking in aluminum welds [5]:

$$U = \left(1 - \frac{K_{op}}{K_{max}}\right)/(1 - R) \tag{7}$$

$$\frac{K_{op}}{K_{max}} = C_0 + C_1 R + C_2 R^2 + C_3 R^3, \tag{8}$$

where

$$C_0 = (0.825 - 0.34\alpha + 0.05\alpha^2)(cos\left(\frac{\pi}{2} \cdot \frac{K_{max}}{K_0}\right)^{\frac{1}{\alpha}}), \tag{9}$$

$$C_1 = (0.415 - 0.071\alpha), \tag{10}$$

$$C_2 = 1 - C_0 - C_1 - C_3, \tag{11}$$

$$C_3 = 2C_0 + C_1 - 1. \tag{12}$$

K_{op} is the SIF caused by the opening stress, σ_{op}, that will result in crack opening when considering the crack closure effect, which is a function of the stress ratio and K_{max}. α is equal to 1 or 3 for plain stress or plain strain conditions respectively. K_0 is the flow stress intensity factor, i.e.,

$$K_0 = \sigma_0 \sqrt{\pi a}, \tag{13}$$

where 'a' is the crack size and σ_0 is the flow stress (average of the yield and ultimate stresses).

4.2. J-Integral Approach

The J-integral method is a path-independent global approach for fracture analysis which provides a means to finding the stress intensity factor for complex geometries. It requires calculating the energy release rate which is a measure of the energy required to propagate a crack. The J-integral is defined as the work performed by the external load on a crack-containing body:

$$J = \int K \, dA, \tag{14}$$

where K is the stress intensity factor along the crack and dA is the incremental area around the crack. The J-integral is calculated by integrating the stress intensity factor along a closed contour surrounding the crack, and it provides a measure of the energy available to drive the crack growth. The J-integral method has several advantages including its ability to consider the effects of stress and deformation around the entire crack, its path independence, and its applications in the presence of crack closure. These advantages make the J-integral method a valuable tool, particularly for structures' complex geometries such as FBG welds.

For linear elastic conditions and Mode 1 cracking, the relationship between the energy release rate and the stress intensity factor can be simplified as follows, where v is Poisson's ratio, which is taken as 0.33, and E is the modulus of elasticity of aluminum, which is taken as 70 GPa:

$$J = K^2 \cdot \left(\frac{1 - v^2}{E}\right). \tag{15}$$

The fatigue life of certain geometries can be predicted numerically by mathematically quantifying the crack propagation rate through linear elastic fracture mechanics (LEFM). However, when working with complex geometries, it is often coupled with a FE analysis to find a solution where a closed-form solution does not exist. For the current paper, a 3D FE model is used to calculate the fatigue life of the specimen using the J-integral method.

4.3. Descriptions of FEA Model

The objective of this portion of the study was to use LEFM to predict the fatigue life of the aluminum T-joints and to conduct a comprehensive analysis of the crack behaviour. Multiple 3D models of the tubular joints associated with 10% increments of weld penetration were constructed to simulate crack growth in loading conditions similar to those applied in the experiments.

Only the portion of the HSS-1 member directly underneath the HSS-2 member (see Figures 1 and 4) was modelled because it was found that meshing the omitted region was too time-consuming. The top of the HSS-2 member was capped as a further simplification and to facilitate load introduction. To further reduce the computational demand of the model, symmetry was leveraged so only a half-model was necessary. The symmetry plane was restrained from translation in the x-axis and rotation about the z-axis (see Figure 4). The exterior surface of the bottom flange and the HSS web were fixed in all degrees of freedom. The top surface of the HSS-2 was constrained to a reference point at its centre to avoid localized deformation at the top surface. This is a simplification of the actual restraint condition which was imposed by a slotted gusset plate connection. Given the distance between the FBG weld and the gusset plate in the actual specimen, it was believed that this simplification would result in improved analysis efficiency with minimal (if any) difference in the predicted stresses in the vicinity of the weld. A pressure load of 0.1778 MPa, which equates to 1 kN applied on a square surface with 75 mm dimensions, was applied to the top surface of the HSS-2 member. The resulting SIF from this applied load can be related to any of the applied load ranges using the principle of superposition, given the elastic nature of the loading. The crack front was defined along the length of the weld propagating outwards as shown in Figure 5.

A meshing technique was used that included a global mesh of half the tube wall thickness (t/2) and a reduced mesh with a circular propagation in the plasticity zone surrounding the crack tip (t/20). The element type used was a quadratic 20-node brick with designation C3D20.

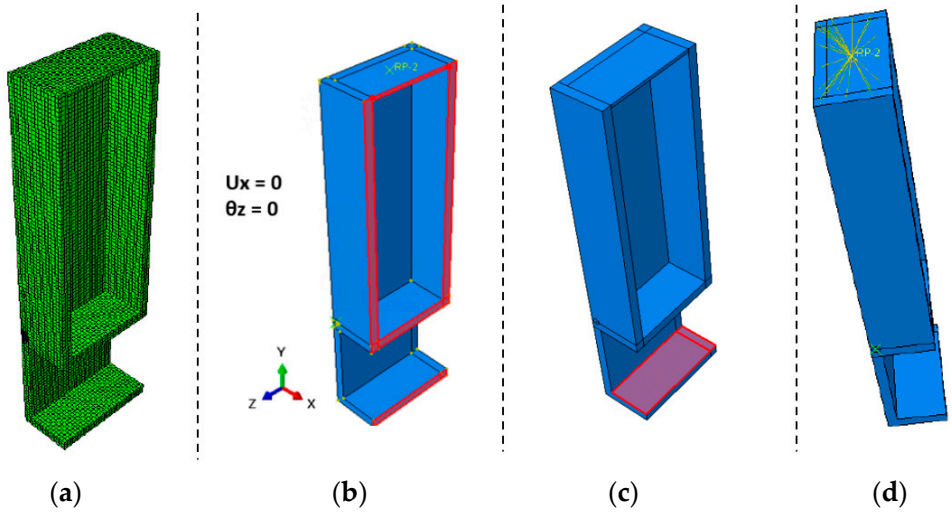

Figure 4. (**a**) ABAQUS 3D half model of the tubes, (**b**) boundary conditions for the surface of symmetry of the half model of the tubes, (**c**) internal surface of HSS-1 is fixed in all degrees of freedom, and (**d**) top surface of HSS-2 where the plate constraint was placed.

4.4. Implementing Paris–Erdogan Crack Growth Law

Table 2 summarizes the parameters that were used in the implementation of the Paris–Erdogan crack growth law, in conjunction with the SIFs obtained from the 3D FE analysis.

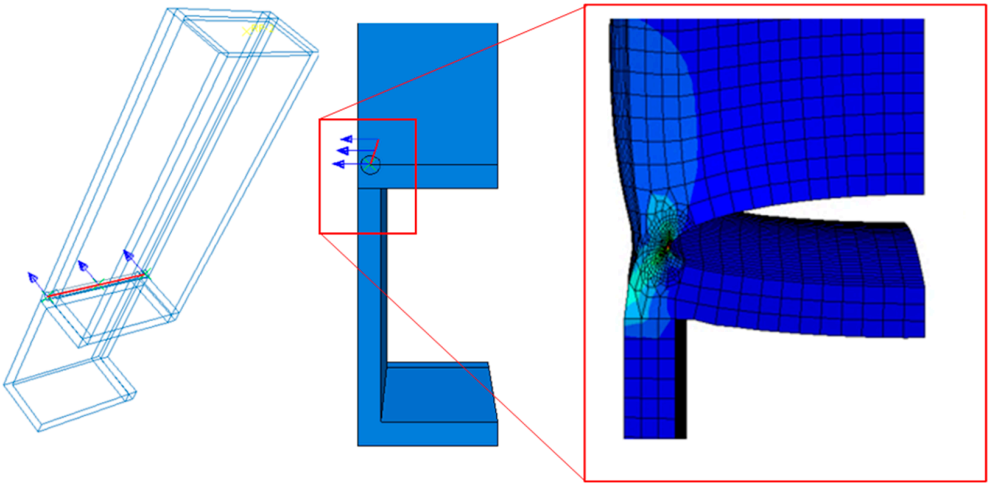

Figure 5. Crack front, assumed crack direction, and mesh in vicinity of FBG weld.

Table 2. Summary of parameters used in LEFM analysis.

Parameter	Value	Units	Reference
σ_y	95	MPa	[10]
σ_u	240	MPa	[10]
σ_o	165	MPa	[14]
C	7.95×10^{-14}	(MPa, mm)	[16]
m	4.0	(MPa, mm)	[16]
ΔK_{th}	$56.7–72.3 \cdot R \geq 21$	MPa$\sqrt{}$mm	[12]

As can be seen in Figure 6, the LEFM (J-integral) analysis produces fatigue life predictions that are conservative in comparison with the line of best fit but lie above the design curve. The conservatism of the modelling process can be attributed to the complex evolution of the actual crack shape which is simplified to a uniform through-crack in the model. Additionally, the model assumes both welds experience the same propagation rate (note that this assumption is implicit in the definition of a plane of symmetry), while the experiments show faster propagation on one side than the other due to slight differences in the weld quality and shape. Additionally, and perhaps more importantly, the LEFM analysis assumes that a crack starts propagating from the lack of fusion tip right from the first load cycle, with no crack initiation phase occurring first.

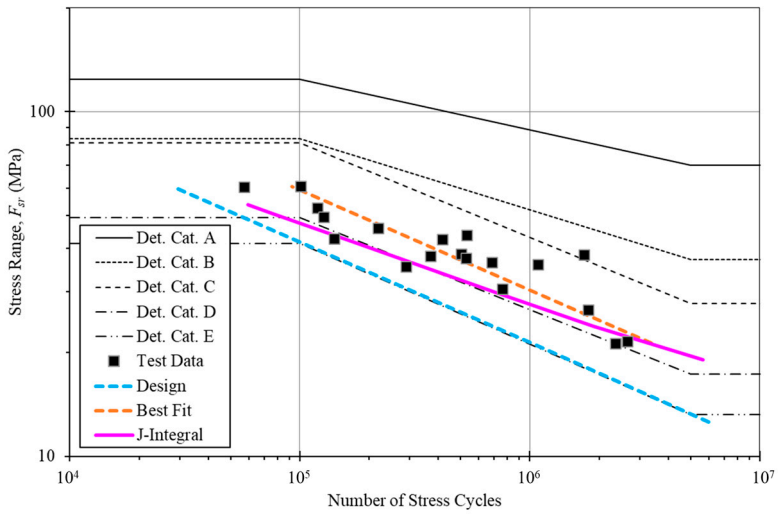

Figure 6. S–N curve showing the design curve obtained from the experimental data and the fatigue life predictions from the LEFM (J-integral) approach.

5. Concluding Remarks

The fatigue testing of 20 T-joint aluminum FBG weld specimens conducted within the scope of this study yielded valuable insights into the fatigue behaviour of this weld type. Notably, the effective throat was found to be the most important factor influencing the performance of the FBG welds and it was found that precision in the welding execution is crucial. An S–N curve was established for a 95% survival probability. The weld performance based on the design curve was found to coincide with Detail Category E in CSA S6-19 when the measured throat was used to calculate the applied stress range. When the design throat was used to calculate the stress range, a lower Detail Category or an adjustment to account for increased uncertainty and differences between the measured and design throat may have been appropriate. A linear elastic fracture mechanics (LEFM)-based approach was then used, along with a 3D finite element (FE) model, to supplement the experimental study and predict the fatigue performance of the tested aluminum FBG welds.

Author Contributions: Conceptualization, A.A. and S.W.; methodology, A.A. and S.W.; validation, A.A.; formal analysis, A.A. and S.W.; investigation, A.A. and S.W.; resources, S.W.; data curation, A.A. and S.W.; writing—original draft preparation, A.A.; writing—review and editing, A.A. and S.W.; visualization, S.W.; supervision, S.W.; project administration, S.W.; funding acquisition, S.W. All authors have read and agreed to the published version of the manuscript.

Funding: Support for this research provided by the NSERC Engage program (Project: 533720-2018) is acknowledged.

Institutional Review Board Statement: Not applicable.

Informed Consent Statement: Not applicable.

Data Availability Statement: Not applicable.

Acknowledgments: Skarborn Engineering is gratefully acknowledged for supporting the collaborative research project that funded the specimen fabrication (through the NSERC Engage program) as well as for providing expertise and assistance with the specimen design and fabrication.

Conflicts of Interest: We declare no conflict of interest.

References

1. Schiller, A.R.; Oswald, M.; Neuhäusler, J.; Rother, K.; Engelhardt, I. Fatigue strength of partial penetration butt welds of mild steel. *Weld. World* **2022**, *66*, 2563–2584. [CrossRef]
2. Kim, S.; Jin, K.; Sung, W.; Nam, S. Effect of Lack of Penetration on the fatigue strength of high strength steel butt weld. *KSME J.* **1994**, *8*, 191–197. [CrossRef]
3. Lawrence, F.V.; Munse, W.H. Fatigue Crack Propagation in Butt Welds Containing Joint Penetration Defects. *Weld. J.* **1973**, *52*, 221–225.
4. Hiroshi, N.; Eto, M.; Tachibana, K.; Nakahira, M. Fatigue strength reduction factor of partial penetration weldments for ITER vacuum vessel. In Proceedings of the SMiRT 16: Selected and Updated Papers from the 16th International Conference on Structural Mechanics in Reactor Technology, Washington, DC, USA, 12–17 August 2001.
5. Laurent, G. Partial Joint Penetration Welds in Aluminum Structures. Master's Thesis, Department of Civil and Environmental Engineering, University of Waterloo, Waterloo, ON, Canada, 2020.
6. Burk, J.; Lawrence, F.V. *Effects of Lack-of-Penetration and Lack-of-Fusion on the Fatigue Properties of 5083 Aluminum Alloy Welds*; Tech. Rep.; University of Illinois at Urbana-Champaign: Champaign, IL, USA, 1976.
7. Brandt, U.; Lawrence, F.V.; Sonsino, C.M. Fatigue crack initiation and growth in AlMg4.5Mn butt weldments. *Fatigue Fract. Eng. Mater. Struct.* **2001**, *24*, 117–126. [CrossRef]
8. Sonsino, C.M.; Radaj, D.; Brandt, U.; Lehrke, H.P. Fatigue assessment of welded joints in AlMg 4.5Mn aluminum alloy (AA 5083) by local approaches. *Int. J. Fatigue* **1999**, *21*, 985–999. [CrossRef]
9. The Aluminum Association. *Aluminum Design Manual*; The Aluminum Association: Arlington County, VA, USA, 2015.
10. CSA. *Strength Design in Aluminum/Commentary on CSA S157-17, Strength Design in Aluminum*; CSA: Seattle, WA, USA, 2018.
11. CSA. *Canadian Highway Bridge Design Code, CSA S6*; CSA: Seattle, WA, USA, 2019.
12. Hobbacher, A.F. *Recommendations for Fatigue Design of Welded Joints and Components*; International Institute of Welding: Genova, Italy, 2014.
13. Paris, P.; Erdogan, F. A critical analysis of crack propagation laws. *J. Basic Eng.* **1963**, *85*, 528–533.
14. Newman, J.C. A crack opening stress equation for fatigue crack growth. *Int. J. Fract.* **1984**, *24*, 131–135. [CrossRef]

15. McClung, R.C. Finite Element Analysis of Specimen Geometry Effects on Fatigue Crack Closure. *Fatigue Fract. Eng. Mater. Struct.* **1994**, *17*, 861–872. [CrossRef]
16. Ranjan, R.; Ghahremani, K.; Walbridge, S.; Ince, A. Testing and fracture mechanics analysis of strength effects on the fatigue behavior of HFMI-treated welds. *Weld. World* **2016**, *60*, 987–999. [CrossRef]